Contents lists available at ScienceDirect

Lithos

journal homepage: www.elsevier.com/locate/lithos



Research Article

A revised interpretation of the Chon Aike magmatic province: Active margin origin and implications for the opening of the Weddell Sea



Joaquin Bastias ^{a,b,*}, Richard Spikings ^a, Teal Riley ^c, Alexey Ulianov ^d, Anne Grunow ^e, Massimo Chiaradia ^a, Francisco Hervé ^{f,g}

- ^a Department of Earth Sciences, University of Geneva, 1205 Genève, Switzerland
- ^b Escuela de Geología, Facultad de Ingeniería, Universidad Santo Tomás, Ejército 146, Santiago, Chile
- ^c British Antarctic Survey, High Cross, Madingley Road, Cambridge CB3 0ET, UK
- ^d Institute of Earth Sciences, University of Lausanne, 1015 Lausanne, Switzerland
- ^e Byrd Polar Research Center, Ohio State University, 108 Scott Hall, 1090 Carmack Road, Columbus, OH 43210, USA
- f Carrera de Geologia, Facultad de Ingenieria, Universidad Andres Bello, 8370106 Santiago, Chile
- g Departamento de Geología, Universidad de Chile, Plaza Ercilla 803, Santiago, Chile.

ARTICLE INFO

Article history: Received 21 April 2020 Received in revised form 22 January 2021 Accepted 22 January 2021 Available online 31 January 2021

ABSTRACT

Late Triassic – Jurassic igneous rocks of the Antarctic Peninsula and Patagonia provide evidence for the evolution of the margin of southwestern Gondwana. We present new geochronological (LA-ICP-MS zircon U—Pb dates) analyses of 12 intrusive and volcanic rocks, which are complemented by geochemical and zircon isotopic (Hf) as well as whole rock isotopic (Nd. Sr.) data. These are combined with similar analyses of 73 other igneous rocks by previous studies, to constrain the magmatic evolution and Late Triassic - Jurassic tectonic setting. The distribution of crystallisation ages reveals four main magmatic pulses that collectively span ~225-145 Ma, all of which have compositions that are consistent with a continental arc setting. The first episode occurred between ~223–200 Ma, and records active margin magmatism within the Antarctic Peninsula and northern Patagonia, and reveals the presence of a flat-slab that gave rise to magmatism in eastern Patagonia. After a period of magmatic quiescence (~200-188 Ma), the second episode occurred between ~188 and 178 Ma, with a continuation of arc magmatism above a flattened slab. The third episode spanned ~173–160 Ma, and its geographic distribution suggests the slab was steepening, driving magmatism towards the south and west in Patagonia. Finally, the fourth period occurred between ~157 and ~ 145 Ma, during which time magmas were emplaced along the Antarctic Peninsula and western Patagonia, with no evidence for flat-slab subduction. The analysed rocks include the Chon Aike magmatic province, which has been considered to have been influenced by the break-up of Gondwana, via heating associated with the Karoo plume in southern Africa and the active margin in western Patagonia and the Antarctic Peninsula. Our new data and revised compilation now suggest that the Early - Middle Chon Aike Jurassic silicic magmatic province in Patagonia and the Antarctic Peninsula can be entirely accounted by active margin processes. We also show that the final stage of Jurassic magmatism (~157-145 Ma) was coincident with rifting that formed oceanic lithosphere of the Weddell Sea and back-arc extension of the Rocas Verdes Basin, potentially revealing the presence of a triple junction located between southern Patagonia and the northern Antarctic Peninsula that led to the disassembly of southern Gondwana.

© 2021 The Author(s). Published by Elsevier B.V. This is an open access article under the CC BY-NC-ND license (http://creativecommons.org/licenses/by-nc-nd/4.0/).

1. Introduction

Most Jurassic magmatism in the southern hemisphere is exposed in Large Igneous Provinces (LIP) that are thought to have been triggered by processes that also disassembled Gondwana. These specific magmatic pulses produced large volumes of igneous rocks in relatively short periods of time and have been used to develop a genetic link between

E-mail address: j.bastias.silva@gmail.com (J. Bastias).

LIPs and the initial stages of continental break-up (e.g. Cox, 1992). The separation of Africa, South America, Antarctica and Australia formed oceanic lithosphere in the late Jurassic, although the earliest magmatism occurred during the Early Jurassic and coincided with the Karoo-Ferrar event (e.g. Elliot and Fleming, 2000; Pankhurst et al., 1998; Riley et al., 2020a), which formed at least two LIPs. These are the Karoo in South Africa (Cox, 1988), the Ferrar (e.g. Storey et al., 2013), which is mostly along the Transantarctic Mountains (Cox, 1992), and potentially also the Chon Aike silicic magmatic province, which is exposed in Patagonia and the Antarctic Peninsula (Pankhurst et al., 1998; Fig. 1). Although some authors have suggested that these

^{*} Corresponding author at:Department of Earth Sciences, University of Geneva, 1205 Genève. Switzerland.

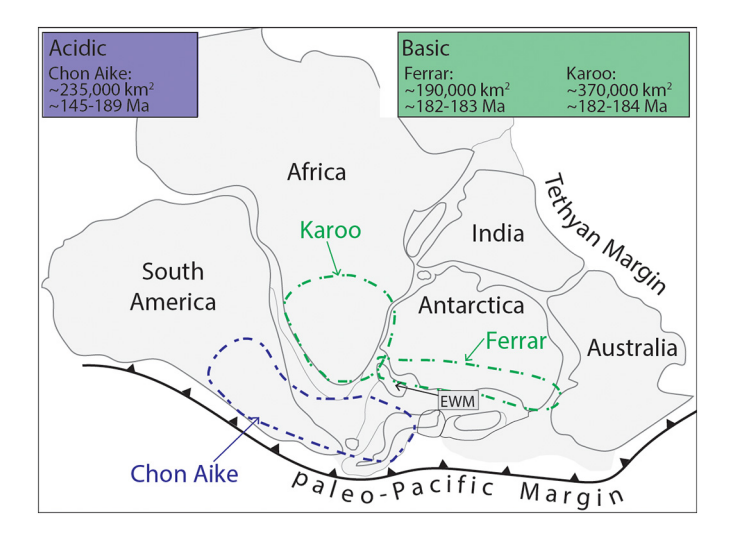


Fig. 1. Paleogeographic reconstruction of the paleo-Pacific active margin of Gondwana during the Late Triassic-Early Jurassic (e.g. Storey et al., 1992, Storey et al., 2001; Lawver et al., 1998; Ghidella et al., 2002; Jokat et al., 2003; Jordan et al., 2017) showing the schematic distribution of the exposures of the acidic Chon Aike (blue) and the basic Karoo and Ferrar (green) LIPs. Estimates of the timing and extension of Chon Aike are from Pankhurst et al. (2000), and this study (new data). The spatial extent of the Karoo and Ferrar LIPs, along with crystallisation ages are from Elliot and Fleming (2004), Sell and Ovtcharova (2014), Burgess et al. (2015) and Svensen et al. (2012).

three provinces are linked through a mantle-plume derived magmatic event (i.e. they are frequently referred to as a continuous but diachronous province; e.g. Storey et al., 2013), they have different crystallisation ages, duration of crystallisation and chemical composition. Alternatively, the Chon Aike magmatic province has been also associated with the subduction of Pacific lithosphere beneath the western margin of Patagonia (e.g. Pankhurst et al., 2000; Rapela et al., 2005; Storey et al., 1992). Furthermore, while the Karoo and Ferrar LIPs host mainly mafic rocks that span ~6 Myr (e.g. Burgess et al., 2015; Greber et al., 2020; Storey et al., 2013; Svensen et al., 2012), the rocks of the Chon Aike magmatic province are mainly felsic and span at least ~35 Myr (e.g. Pankhurst et al., 2000; Riley et al., 2001). We show that it is not necessary to invoke the involvement of the mantle-plume to form the magmatic rocks of the Chon Aike magmatic province in the Antarctic Peninsula and Patagonia.

Geochemical and isotopic data of the volcanic rocks of the Karoo-Ferrar are generally interpreted to be indicative of an origin associated with a thermal anomaly in the Earth's mantle (Duncan and Richards, 1991; White and McKenzie, 1989). However, the mechanisms that initiated this thermal event remain enigmatic (e.g. Storey et al., 2013). Possible explanations include supercontinent insulation (e.g. Coltice et al., 2007), thermal upwelling of mantle-sources within a mantle plume (Richards et al., 1989), plume capture (Dalziel et al., 2000) and decompression related to plate tectonic processes (e.g. Elkins-Tanton, 2005). The geographic distribution of the acidic Chon Aike magmatic province has been explained as a combination of the peripheral thermal effect of the Karoo mantle plume from Africa and active margin processes along western Patagonia and the Antarctic Peninsula (e.g. Pankhurst et al., 2000; Riley et al., 2001; Storey et al., 1992). Although the heat required to initiate bulk crustal fusion may have been supplied by a mantle plume, direct evidence for the involvement of the mantle remains obscure and has been a focus of debate since early research that linked LIPs with continental break-up (Hawkesworth et al., 1999). Here we re-evaluate the origin of the Chon Aike magmatic province using new geochemical and isotopic data acquired from Late Triassic-Jurassic igneous rocks of the Antarctic Peninsula. Our data are combined with

previous geochronological, isotopic and geochemical data from Patagonia and the Antarctic Peninsula that have been filtered for accuracy. Our compilation includes whole rock major and trace element compositions, U/Pb zircon dates, 40 Ar/ 39 Ar hornblende dates, and whole rock (Sr, Nd) and zircon (Hf) isotopic tracing. We conclude that the igneous rocks of the Chon Aike magmatic province formed above an active margin without the necessity to invoke the involvement of a mantle plume.

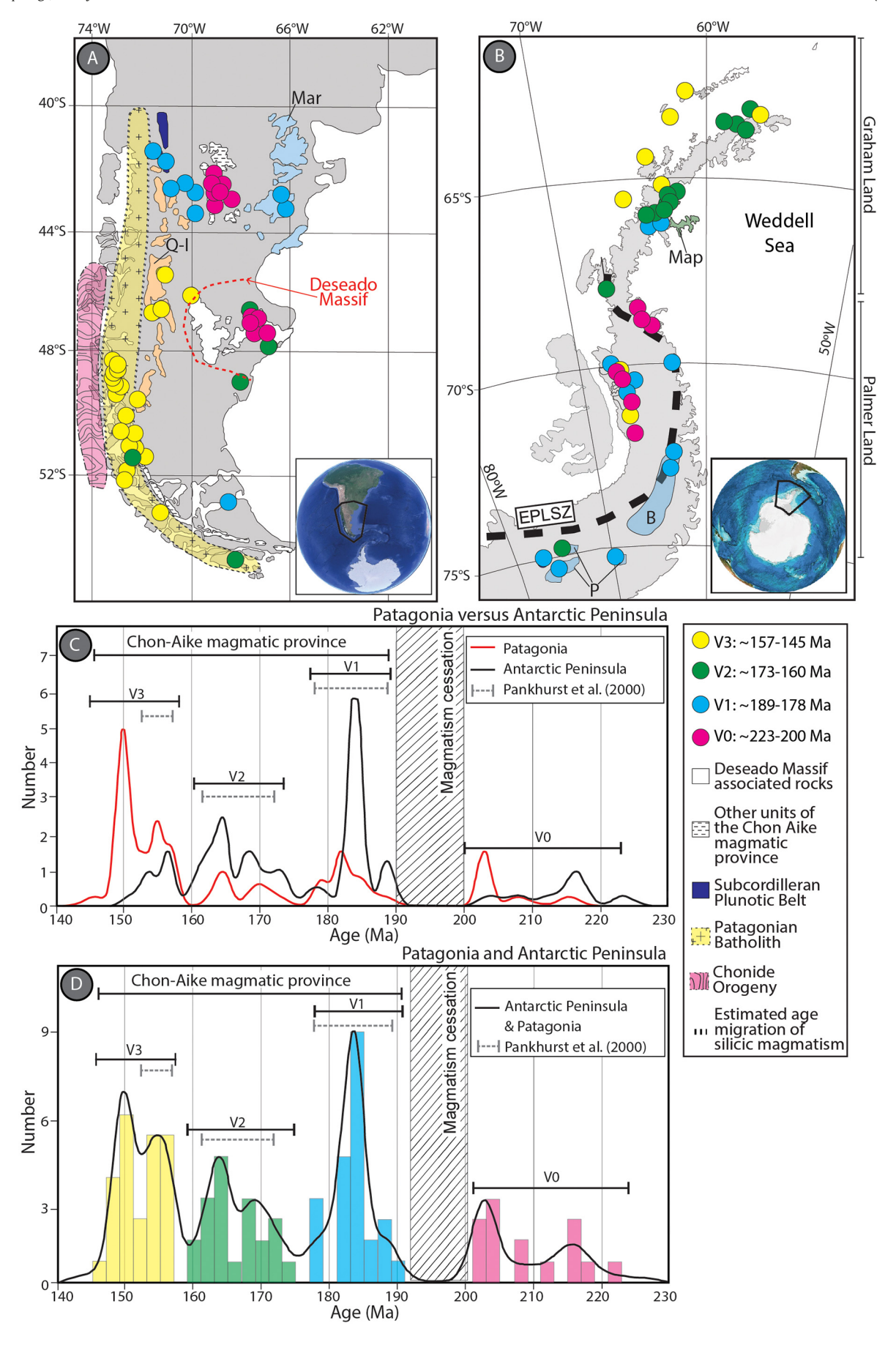
2. Geological framework

2.1. The Karoo, Ferrar and Chon Aike magmatic provinces

The mafic igneous rocks of the Karoo and Ferrar provinces crop out in southern Africa-East Antarctica-Mozambique, and the Transantarctic Mountains-South Australia-New Zealand regions (Fig. 1). Despite minor geochemical differences (e.g. Elliot and Fleming, 2000; Riley, 2006), the rocks yield ages that reveal magmatic peaks that are closely spaced in time (between 183.36 \pm 0.17/0.27 to 183.06 \pm 0.07/0.21 Ma for the Karoo basin sills and 182.85 \pm 0.35 and 182.43 \pm 0.06 Ma for Ferrar; zircon U—Pb geochronology; Svensen et al., 2012; Burgess et al., 2015; Greber et al., 2020). The Chon Aike magmatic province is exposed along major tracts of Patagonia and the Antarctic Peninsula (Fig. 1; Pankhurst et al., 1998). Exposures are dominated by volcanic silicic rocks, with minor mafic and intermediate igneous rocks (Pankhurst et al., 1998, 2000; Riley et al., 2001). The rocks of the Chon Aike magmatic province have yielded ages that have been interpreted to span more than ~35 Myr of magmatic activity (~188-153 Ma; zircon ²⁰⁶Pb—²³⁸U, whole-rock Rb—Sr and feldspar ⁴⁰Ar/³⁹Ar; Féraud et al., 1999; Pankhurst et al., 2000). Pankhurst et al. (2000) identified three main temporal magmatic pulses, which are V1 (188-178 Na), V2 (172–162 Ma) and V3 (157–153 Ma). The exposures in Patagonia of the V1 and V2 episodes are mostly present in eastern and central Patagonia (Fig. 2a), while the V3 episode dominates the western margin (Fig. 2a). The exposures of these episodes in the Antarctic Peninsula are dispersed along a north-south axis, where the V1 episode is found in the south (Palmer Land) and the V2 and V3 episodes are exposed in the north (Graham Land; Fig. 2b). Several authors have noted that the timing of V1 brackets the peak of the Karoo-Ferrar event at 183 \pm 1 Ma (Encarnacion et al., 1996; Riley, 2006). This contemporaneity has been a major factor when genetically linking the Karoo and Ferrar LIPs with the Chon Aike magmatic province (Pankhurst et al., 2000). Combined major and trace element abundances with whole-rock isotopic data (Sr-Nd-O) suggests that the V1 and V2 magmas formed by anatexis of Grenvillian-aged, mafic, lower crustal rocks, which subsequently evolved by assimilation and fractionation (Pankhurst and Rapela, 1995; and Riley et al. (2001). Seitz et al. (2018) utilised O-isotope to suggest partial melting of continental crust was the main mechanism that formed the Chon Aike magmatic province. V1 magmas were considered to be melts of upper-crustal paragneiss that mixed with lower crustal melts in magma chambers in the upper crust, whereas V2 magmas formed by assimilation-fractional crystallisation of isotopically uniform magma in upper-crustal magma chambers. Riley et al. (2001) suggested that these magmas are either related to the Karoo group of plumes and/or to the presence of highly fusible crust in a long-lived continental active margin.

2.2. Active margin magmatism in Patagonia and the Antarctic Peninsula during the Late Triassic-Jurassic

Navarrete et al. (2019) and Bastias et al. (2020) recently suggested that the Gondwanan margin of the Antarctic Peninsula-Patagonia region was active during the Late Triassic, which is consistent with the interpretations of Millar et al. (2002) and Vaughan et al. (2012). Bastias et al. (2020) showed report that Late Triassic orthogneisses of the Rymill Granite Complex in the Antarctic Peninsula reveal an active margin along the south-central Antarctic Peninsula, which had probably been



active since the Late Palaeozoic. Recently, Riley et al. (2020b) reported that the rocks of the Rymill Granite Complex record a magmatic episode at ~227 Ma, followed of a metamorphic overgrowths at ~207 Ma. Navarrete et al. (2019) suggested that Late Triassic igneous rocks of the Deseado Massif in eastern Patagonia also formed above an active margin. The Deseado Massif is currently located ~1000 km inland from the hypothetical paleo-trench (Fig. 2a), which implies a phase of Late Triassic flat-slab subduction that has been referred to as the South Gondwanan flat-slab (Navarrete et al., 2019).

Jurassic magmatism is geographically widespread in Patagonia and the Antarctic Peninsula, with exposures spanning from the Atlantic margin to the Pacific margin in Patagonia (Fig. 2a), and almost covering a complete north-south length of the continental crust of the Antarctic Peninsula (Fig. 2b) and Patagonia (Fig. 2a). Previous studies of Jurassic magmatism suggested that the igneous rocks in western Patagonia and the northern Antarctic Peninsula are subduction-related, whereas those in eastern Patagonia and the southern Antarctic Peninsula are either derived from mantle-plume activity, or formed due to extension and thinning during the disassembly of Gondwana (e.g. Pankhurst et al., 2000; Riley et al., 2001; Storey et al., 1992). Active margin magmatism along western Patagonia includes the Subcordilleran Plutonic Belt (Rapela et al., 2005), the Patagonian Batholith (Pankhurst et al., 1992; Hervé et al., 2007), and the V3 Chon Aike episode (Pankhurst et al., 2000). Some of these units have been correlated with rocks present in the Antarctic Peninsula (e.g. Riley et al., 2001, 2017). The plume-influenced igneous rocks includes the V1 and V2 Chon Aike, and these have been divided into several formations that are located in eastern and central Patagonia, and in the southern and central Antarctic Peninsula (e.g. Pankhurst et al., 2000). The involvement of a mantle plume was considered by some authors (e.g. Pankhurst et al., 2000; Riley et al., 2001) due to voluminous silicic volcanism in an extensional setting, and the juxtaposition of coeval rocks of the Chon Aike magmatic province with the mantle plume-related Karoo and Ferrar LIPs. Here we define two regions, which are, (i) the Western Margin, which includes rocks of the Subcordilleran Plutonic Belt, the Patagonian Batholith, V3 Chon Aike episode and the V1 and V2 Chon Aike units in the Antarctic Peninsula, and (ii) the Inland Region, which includes exposures of the V1 and V2 Chon Aike episodes from Eastern Patagonia. These definitions facilitate a comparison of inland versus classic arc rocks (i.e. Western Margin) that commonly form within ~300 to 100 km of the trench.

3. Methods

We present a compilation of geochronological, geochemical and isotopic analyses that includes new data and relevant previous work. While we have new data from the Antarctic Peninsula, we have incorporated previous work from Patagonia and the Antarctic Peninsula. Previous geochronological data was filtered for concordance (U—Pb) and the topology of age spectra (40 Ar/ 39 Ar data). This was necessary due to the ubiquitous presence of alteration products in the region (e.g. Bastias et al., 2016; Leat et al., 2009).

Data are presented from 12 igneous rocks from the Antarctic Peninsula that were loaned by the British Antarctic Survey and the Polar Rock Repository at Ohio State University (Table 1). The detailed methodology and full dataset has been presented in Bastias et al. (2021).

4. Results

4.1. Geochronology

Early attempts to date the Triassic-Jurassic rocks in Patagonia and the Antarctic Peninsula utilised the K/Ar, Rb/Sr and 40Ar/39Ar methods (e.g. Rex, 1976), resulting in a large scatter of dates due to variable degrees of daughter isotope loss. We present (Fig. 2) a geochronological dataset for Patagonia (Fig. 2a) and the Antarctic Peninsula (Fig. 2b) that combines robust results from previous work and our new data from volcanic and plutonic rocks of the Antarctic Peninsula. Our new ²⁰⁶Pb—²³⁸U zircon concordia ages (LA-ICP-MS) of four volcanic rocks range between 179 \pm 1 Ma and 161 \pm 1 Ma, while eight intrusions yield ages between 183 \pm 1 and 151 \pm 1 Ma. These results are combined with 74 U-Pb zircon concordia ages obtained using TIMS, SHRIMP and LA-ICP-MS, and five previous 40Ar/39Ar plateau dates from Patagonia and the Antarctic Peninsula from previous work (Bastias, 2020; Bastias et al., 2019; Bastias et al., 2020; Calderón et al., 2007; Fanning et al., 1997; Hervé et al., 2007; Leat et al., 2009; Lovecchio et al., 2019; Mukasa and Dalziel, 1996; Navarrete et al., 2019; Pankhurst et al., 2000; Rapela et al., 2005; Riley et al., 2012, 2016). The distribution of ages reveals four main magmatic pulses that collectively span ~225-145 Ma (Figs. 2c, d). The oldest magmatic pulse, which we refer to as V0, spans ~223-200 Ma and includes the Rymill Granite Complex in the Antarctic Peninsula (Bastias et al., 2020; Riley et al., 2020b), and the Calandria Formation of the Deseado Massif in eastern Patagonia (e.g. Navarrete et al., 2019; Pankhurst et al., 1993). This period is followed by magmatic quiescence during ~200-190 Ma. The timing of younger magmatism is only mildly different to the V1, V2 and V3 pulses defined by Pankhurst et al. (2000) for the Chon Aike magmatic province. We have slightly modified the time limits of the previous magmatic pulses that were defined by Pankhurst et al. (2000), although we continue to refer to these as V1, V2 and V3. Our kernel density estimations suggest that these pulses were active during ~188-178 Ma (V1; revised from ~188-178 Ma; Pankhurst et al., 2000), ~173-160 Ma (V2; revised from ~172-162 Ma; Pankhurst et al., 2000) and ~ 157-145 Ma (V3; revised from ~157-153 Ma; Pankhurst et al., 2000). The general distribution of ages in the Antarctic Peninsula broadly reveals a northward migration of magmatism that was first proposed by Pankhurst et al. (2000; Fig. 2b). The distribution of ages in the southern Antarctic Peninsula is dominated by the two oldest episodes (V0, ~220-200 Ma and V1, ~188-175 Ma; Fig. 2b), while the two youngest episodes are found in the northern Antarctic Peninsula (V2, ~172-162 and V3, ~157-154 Ma; Fig. 2). The geographic distribution of episodes V0, V1 and V2 in Patagonia reveals an approximate east-west scatter of temporally overlapping magmatism at similar latitude (Fig. 2a), which partially agrees with the migration of magmatism towards the western margin, as suggested by the previous studies (e.g. Pankhurst et al., 2000; Riley et al., 2001; Storey et al., 2013).

4.2. Major and trace element geochemistry

4.2.1. V0 episode (~223-200 Ma)

The Late Triassic VO episode includes plutonic rocks of the Rymill Granite Complex of the Antarctic Peninsula (Western Margin; Bastias

Fig. 2. Zircon ²⁰⁶Pb—²³⁸U concordia and ⁴⁰Arj³⁹Ar plateau ages of the Antarctic Peninsula and Patagonia during the Late Triassic-Jurassic (see also Table 1). The dates define four magmatic episodes: ~223–200 Ma (pink), ~189–178 Ma (light blue), ~173–160 Ma (green) and ~157–145 Ma (yellow). (A) Map of present day Patagonia showing the geochronological results. Q-I: El Quemado and Ibanez formations, Mar; Marifil Formation. The geographical extent of the Chonide Orogeny is from Thomson and Hervé (2002), Sepúlveda et al. (2008) and Willner et al. (2009). (B) Map of the present day Antarctic Peninsula showing the geochronological results. B: Brennecke Formation, EPLSZ: Eastern Palmer Land Shear Zone (EPLSZ; Vaughan & Storey, 2000), Map: Mapple Formation, P: Mount Poster Formation. (C) Kernel density estimates of the distribution of U—Pb concordia and Ar/Ar plateau dates. Revised estimates of the time of the Chon Aike episodes V0-V3 in brackets (D) Kernel density estimates of the distribution of crystallisation ages within the combined dataset acquired from the Antarctic Peninsula and Patagonia. Data sources: Riley et al. (2001); Rapela et al. (2005); Hervé et al. (2007); Navarrete et al. (2019), Bastias et al. (2020a, 2020b) and this work. Dates are binned into 2 My intervals. A detailed methodology and full dataset is presented in Bastias et al. (2021).

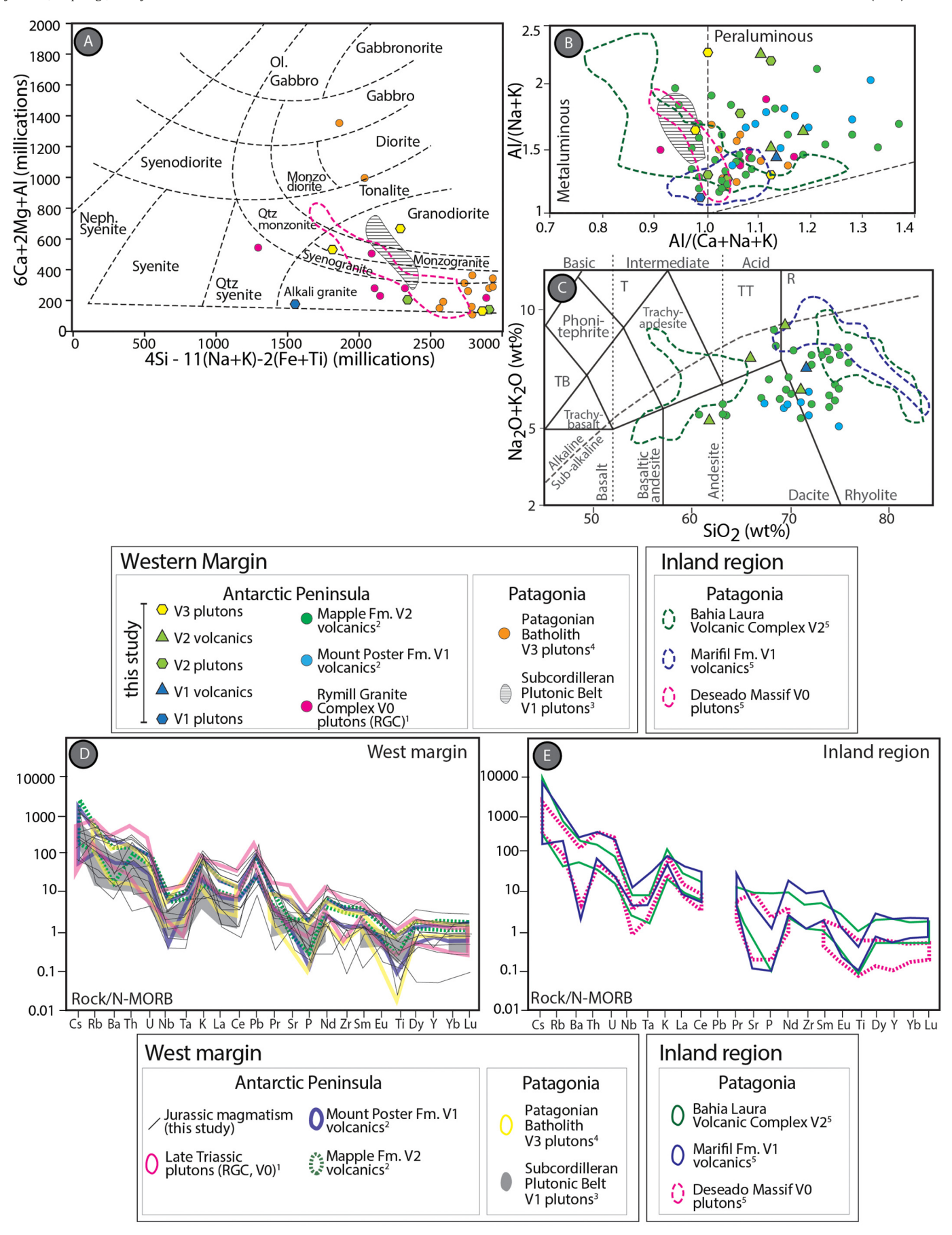
Table 1Major oxide and trace element, including REE and isotopic tracing data from selected rocks of the Antarctic Peninsula.

Code	PRR-5983	PRR-6037	PRR-32977	PRR-6230	R.6569.9	R.6871.3	R.6607.1	R.6602.3	R.5957.3	R.5257.5	R.6307.1	R.6851.1
Internal Code	15JB72	15JB73	16JB69	16JB70	18JB01	18JB04	18JB05	18JB07	18JB26	18JB32	18JB50	18JB52
Age	163	156	160	151	164	179	162	165	156	183	153	161
Error	3	2	2	1	2	2	2	1	3	8 H Db 7:	1	1
Method	U-Pb Zr 63.55	U-Pb Zr 68.18	U-Pb Zr 63.42	U-Pb Zr 65.43	U-Pb Zr	U-Pb Zr 75.19	U-Pb Zr	U-Pb Zr	U-Pb Zr 70.70	U-Pb Zr	U-Pb Zr	U-Pb Zr 65.40
South West	-63.33 -58.93	-68.18 -67.00	-63.42 -57.01	-65.48	-65.60 -62.50	-75.19 -71.42	-65.53 -62.43	-65.53 -62.20	-70.70 -67.57	-70.03 -67.65	-71.58 -66.89	-63.40 -62.70
SiO ₂	-38.93 71.44	70.20	76.44	62.37	76.83	71.05	-02.43 71.71	61.66	73.96	70.23	62.05	65.98
TiO ₂	0.36	0.16	0.16	1.12	0.29	1.07	0.40	0.01	0.46	0.14	0.79	0.63
Al_2O_3	15.39	12.98	12.16	15.33	12.17	12.94	15.13	16.17	14.53	14.79	15.84	16.32
Fe ₂ O ₃	2.83	1.71	1.97	6.96	1.69	4.53	2.80	7.29	3.06	1.44	6.76	4.01
MnO	0.04	0.04	0.04	0.09	0.06	0.08	0.05	n.d.	0.05	0.01	0.13	0.06
MgO	0.55	0.34	0.46	2.75	0.27	1.73	0.64	1.77	0.78	0.07	2.16	1.13
CaO	3.17	1.37	0.43	3.43	0.98	1.30	1.90	4.22	3.45	0.52	4.87	2.07
Na ₂ O	3.26	3.15	3.93	4.82	2.61	3.34	3.35	2.01	3.52	2.06	2.91	2.76
K ₂ O	3.08	4.83	3.28	1.36	5.20	3.33	4.24	3.44	0.80	9.85	1.96	5.09
$P_{2}O_{5}$	0.08	0.04	0.02	0.19	0.04	0.25	0.10	0.19	0.05	0.22	0.16	0.15
Cr ₂ O ₃	n.d.	n.d.	0.01	n.d.	n.d.	0.01	0.01	0.01	0.01	n.d.	0.01	n.d.
LOI	0.91	5.18	0.84	1.56	0.64	1.26	0.87	2.51	0.63	0.28	1.21	1.41
Total	100.21	94.81	98.89	98.42	100.12	99.63	100.33	96.79	100.66	99.33	97.63	98.21
Be	2.96	3.19	2.46	1.68	5.19	2.68	3.83	1.30	2.31	0.93	2.54	3.25
Sc	16.88	17.61	13.52	25.66	13.62	19.64	15.38	11.74	10.17	8.59	22.28	16.81
Ni	7.88	11.82	3.79	9.18	7.44	16.36	8.90	3.91	4.88	7.39	3.14	5.49
Cu	9.66	77.12	6.96	17.60	13.60	11.83	5.49	5.75	6.83	4.27	15.79	16.90
Zn Rb	40.63 101.93	54.89 93.51	40.24 101.38	45.77 30.03	115.08 341.91	87.59 87.02	65.99 153.42	20.62 5.74	45.73 19.78	16.82 234.73	80.99 73.85	61.37 156.47
Sr	287.66	247.71	96.26	302.69	59.32	58.97	210.13	156.84	202.56	272.38	290.42	228.14
Y	16.46	26.74	26.55	36.55	43.10	49.65	27.61	6.21	2.94	42.97	24.02	22.36
Zr	111.64	101.79	145.49	200.76	120.94	375.21	160.10	14.03	166.94	11.38	155.80	248.73
Nb	9.04	9.10	8.49	4.31	11.23	17.75	9.97	4.24	1.49	2.62	7.87	11.33
Mo	0.49	1.03	0.76	0.42	1.14	0.88	1.24	0.75	1.05	0.51	0.84	0.57
Cs	2.27	2.19	0.58	0.68	8.59	1.47	1.49	5.61	0.79	0.53	1.95	4.97
Ba	750.59	304.33	740.92	135.38	290.82	621.33	745.48	24.41	239.11	1976.30	647.25	1144.29
La	23.33	22.22	92.98	16.66	37.38	54.46	37.43	5.64	5.85	7.50	26.13	41.12
Ce	49.86	47.90	163.19	38.69	87.55	114.64	77.64	5.75	9.88	17.79	50.04	80.83
Pr	5.29	5.71	18.14	4.96	9.00	13.17	8.51	3.61	0.94	2.57	5.78	8.97
Nd	19.69	23.25	66.87	22.78	33.73	53.44	33.02	5.70	3.38	13.08	23.65	34.50
Sm	3.83	5.02	9.78	5.62	7.14	10.65	6.40	3.82	0.63	4.57	4.77	6.21
Eu	1.01	0.72	0.93	1.46	0.39	1.53	0.93	1.81	0.85	1.70	1.15	1.56
Gd	3.55	4.68	7.13	5.89	6.57	10.02	5.57	3.66	0.58	6.25	4.52	5.12
Tb	0.53	0.72	0.86	0.92	1.05	1.45	0.80	0.84	0.07	1.22	0.66	0.69
Dy	3.41	4.81	5.33	6.55	7.44	9.41	5.24	3.25	0.50	7.86	4.34	4.27
Но	0.69	0.98	0.93	1.32	1.49	1.85	1.00	1.00	0.10	1.60	0.88	0.82
Er Tm	1.88	2.86	2.67	4.02	4.36	5.26	2.93	2.18	0.33	4.72	2.55	2.33
Yb	0.26 1.79	0.44 3.09	0.38 2.68	0.61 4.34	0.65 4.48	0.71 5.03	0.43 2.91	0.43 2.16	0.06 0.47	0.61 4.24	0.38 2.66	0.33 2.27
Lu	0.28	0.45	0.38	0.64	0.63	0.72	0.42	0.44	0.47	0.58	0.40	0.36
Hf	2.93	3.70	4.47	5.36	3.91	9.97	4.78	3.33	4.26	0.41	4.04	6.64
Ta	0.59	0.72	0.70	0.31	1.42	1.31	0.91	0.70	0.09	0.15	0.51	0.68
W	0.27	1.76	0.81	0.42	10.72	2.93	2.23	2.33	0.84	0.12	0.21	2.05
Pb	14.53	15.06	22.48	7.33	43.87	22.16	21.92	7.37	4.48	66.35	12.20	15.21
Th	7.55	11.01	18.64	4.65	26.22	18.35	16.35	2.84	0.73	1.65	6.34	12.30
U	0.92	2.24	2.87	1.34	2.98	3.28	3.21	1.31	0.34	0.74	1.79	2.40
Co	4.13	n.d.	1.14	15.97	3.89	10.78	5.55	11.43	5.52	0.97	13.61	5.41
Fe#	0.85	0.82	0.80	0.70	0.85	0.70	0.80	0.79	0.78	0.96	0.78	0.80
A/CNK	1.06	1.01	1.13	0.98	1.04	1.13	1.12	1.10	1.12	0.99	1.00	1.18
A/NK	1.77	1.25	1.21	1.63	1.23	1.42	1.50	2.30	2.18	1.05	2.29	1.62
Y + Nb	25.50	35.84	35.04	40.86	54.34	67.40	37.58	10.44	4.43	45.59	31.89	33.69
Sr/Y	17.48	9.26	3.63	8.28	1.38	1.19	7.61	25.27	68.90	6.34	12.09	10.20
Rb/Y	6.19	3.50	3.82	0.82	7.93	1.75	5.56	0.92	6.73	5.46	3.07	7.00
87 Sr/ 86 Sr _i	n.d.	0.7084	0.7074	0.7044	n.d.	0.7200	0.7081	0.7089	0.7042	0.7125	0.7079	0.7082
εNdi	n.d.	-2.57	-4.06	3.85	-2.64	-7.73	-3.70	-8.62	3.43	-0.28	-3.49	-3.64

n.d.: no data.

et al., 2020) and the Late Triassic Deseado Massif in eastern Patagonia (Inland Region; Pankhurst et al., 1993; Rapela and Pankhurst, 1996; Navarrete et al., 2019). Plutonic rocks of the Rymill Granite Complex are mainly alkali granites with minor monzogranites and quartz-syenites, according to the multi-cation discrimination classification scheme of de La Roche et al. (1980; Fig. 3a). Similarly, Late Triassic intrusions within the Deseado Massif are dominantly alkali granites with some syenogranites, diorites, monzogranites and tonalites (Fig. 3a). The Rymill Granite Complex and the Deseado Massif yield

metaluminous and peraluminous Aluminum Saturation Indices (ASI) of 1.16–0.91 and 1.03–0.91, respectively (Fig. 3b). These ASI values define metaluminous and peraluminous compositions, although the Late Triassic Deseado Massif also hosts rocks that yield peralkaline compositions. N-MORB normalised trace element abundances of the Rymill Granite Complex show an enrichment in Light Ion Lithophile Elements (LILE), with negative Nb, Ta, Sr, P and Ti anomalies, suggesting that a subduction derived component is incorporated into these rocks, and that they may have formed within a continental arc (Fig. 3d). Minor



negative Ba, Eu and Sr anomalies, combined with a strong negative Ti anomaly, suggest that plagioclase and Fe—Ti oxides have fractionated, and the positive Pb anomaly is likely to have been derived from an upper crustal source. N-MORB normalised trace element abundances of the Late Triassic Deseado Massif (Fig. 3e) are extremely similar to the Rymill Granite Complex.

4.2.2. V1 episode (~188-178 Ma)

Igneous units of the V1 episode are exposed along the southern Antarctic Peninsula and in western and eastern Patagonia (Fig. 2a, b). Exposure of the plutonic record is limited compared to volcanic exposures, and is present in the Subcordilleran Plutonic Belt of western Patagonia (Rapela et al., 2005) and in the southern Antarctic Peninsula, from where we present new geochemical data (alkali granite with the R.5257.5; Fig. 3a). The volcanic rocks are mostly part or associated to the V1 Chon Aike magmatic province (e.g. Pankhurst et al., 2000; Riley et al., 2001, 2017, 2020a), and we include geochemical data from the Marifil Formation of eastern Patagonia (Inland Region; Navarrete et al., 2019) and the Mount Poster Formation of the southern Antarctic Peninsula (Western Margin; Riley et al., 2001). The rocks of the Mount Poster Formation are rhyolites and dacites, whereas coeval volcanic rocks of the Marifil Formation are rhyolites (Fig. 3c). Major element compositions designate the plutonic rocks of the Subcordilleran Plutonic Belt in western Patagonia as granodiorites, monzogranites and minor syenogranites (Fig. 3a). Aluminum Saturation Indices of the Mount Poster Formation of the Antarctic Peninsula, and the Marifil Formation of eastern Patagonia span between 1.31 and 0.70 and 1.12-0.94, respectively (Fig. 3b). The rocks of the Subcordilleran Plutonic Belt of western Patagonia and alkali granite R5257.5 of the Antarctic Peninsula have metaluminous compositions (Fig. 3b), N-MORB normalised trace element abundances of the Western Margin reveal enriched LILE and Pb abundances, and negative Nb, Ta, Sr, P and Ti anomalies (Fig. 3d), which suggest the incorporation of subduction-related material into these rocks. These include the Subcordilleran Plutonic Belt of western Patagonia (Rapela et al., 2005) and the Mount Poster Formation of the V1 Chon Aike episode in the Antarctic Peninsula (Riley et al., 2001). The Marifil Formation of the Inland Region of eastern Patagonia yields similar geochemical compositions to the Western Margin (Fig. 3e; Navarrete et al., 2019). V1 magmatism in the Western Margin and the Inland Region have extremely similar geochemical characteristics, and they probably formed within a continental active margin (Fig. 3).

4.2.3. V2 episode (~173-160 Ma)

V2-aged rocks are mostly found within the V2 Chon Aike magmatic province, which occurs in the northern Antarctic Peninsula and in central and eastern Patagonia (Fig. 2). We present new geochemical data from three plutonic and four volcanic rocks of the Antarctic Peninsula that crystallised during the V2 episode (Table 1). These units do not form part of an a priori classified rock formation and remain stratigraphically unclassified. We combine these results with published work from the Mapple Formation of the northern Antarctic Peninsula (e.g. Riley et al., 2001, 2010) and the Bahia Laura Volcanic Complex of eastern Patagonia (Navarrete et al., 2019), which correspond to the Western Margin and Inland Region magmatism, respectively. Major element abundances designate the rocks of the Mapple Formation (Riley et al., 2001) as dacites and rhyolites, with minor andesites (Fig. 3c). The new data yield alkali granite, monzogranite (Fig. 3a), rhyolite, dacite and andesite compositions (Fig. 3c), which is consistent with the

lithologies reported from the Mapple Formation. The volcanic rocks of the Bahia Laura Volcanic Complex in eastern Patagonia yield bi-modal compositions defined by rhyolites (>75% wt% SiO₂) and basalticandesites, and andesites with minor dacites and trachy-andesite (<68% wt% SiO₂). ASI values of the volcanic and plutonic rocks in the new dataset yield peraluminous compositions, with values of 1.18 to 1.10, and 1.12 to 1.01, respectively (Fig. 3b). These overlap with ASI values obtained from the Mapple Formation of the Antarctic Peninsula, which span between 1.36 and 0.94. The volcanic rocks that define the Inland Region (Bahia Laura Volcanic Complex in eastern Patagonia) yield ASI values that range between 1.24 and 0.70 (Fig. 3b), overlapping with the compositions of coeval, V2 volcanic and plutonic rocks of the Western Margin. N-MORB normalised trace element abundances of the V2 episode are indistinguishable from the Inland Region (Fig. 3e; Bahia Laura Volcanic Complex) and the Western Margin (Fig. 3d; Mapple Formation in the Antarctic Peninsula and the new data), and are characterized by negative Ti, Nb and Ta anomalies with enriched LILE and Pb abundances (Figs. 3d, e). Similar to V0 and V1-aged rocks, these geochemical features suggest the inclusion of a subductionderived component in V2-aged magmatism, and these rocks probably formed in an active margin setting.

4.2.4. V3 episode (~157–145 Ma)

Episode V3 only includes intrusions that are exposed along the western margin of Patagonia and the Antarctic Peninsula, and thus this period is missing in the Inland Region. We present new geochemical data from three plutonic rocks of the Antarctic Peninsula, which yield syenogranite, granodiorite and alkali granite compositions according to their major element abundances (Fig. 3a). Previous geochemical studies were restricted to the Patagonian Batholith in western Patagonia (Hervé et al., 2007). This unit is mainly composed of alkali granites and minor syenogranites, diorites and gabbros (Fig. 3a), rendering it similar to the new V3 intrusions in the Antarctic Peninsula. V3-aged plutons of the Antarctic Peninsula are peraluminous and metaluminous with ASI values ranging between 1.13 and 0.98, which overlap with those obtained from the Patagonian Batholith, which span between 1.16 and 0.81 (Fig. 3b). N-MORB normalised trace element abundances of the V3 intrusions (Fig. 3d) are extremely similar to those obtained from igneous rocks of the V0, V1 and V2 episodes, and corroborate previous reports that the V3-aged rocks formed above an active margin (e.g. Hervé et al., 2007).

4.3. Sr—Nd bulk rock isotopes

Whole rock, time-corrected Sr—Nd isotopic compositions of the Late Triassic – Jurassic igneous rocks of the Patagonia-Antarctic Peninsula region are presented in Fig. 4 (summarized in a and b). Isotopic data from episode V0 (Fig. 4 c and d; ~223–200 Ma) was obtained from the Rymill Granite Complex along the western margin (Bastias et al., 2020), and the plutons of the Deseado Massif located in eastern Patagonia (Rapela and Pankhurst, 1996). These intrusions yield Nd isotopic compositions that are less radiogenic than CHUR (e.g. Bouvier et al., 2008; Fig. 4a), with ϵ Nd_i values that range between -6.2 and -0.3, and radiogenic ϵ 7Sr/ ϵ 6Sr ratios of 0.714–0.705 compared to the present-day depleted mantle (ϵ 7Sr/ ϵ 6Sr ϵ 0.702; Zindler and Hart, 1986; Fig. 4b).

Volcanic and plutonic rocks that crystallised during the V1 episode (Fig. 4 e and f; ~188–178 Ma) along the Western Margin and Inland Region yield highly varied ϵNd_i and ${}^{87}Sr_i{}^{86}Sr_i$ values that range between

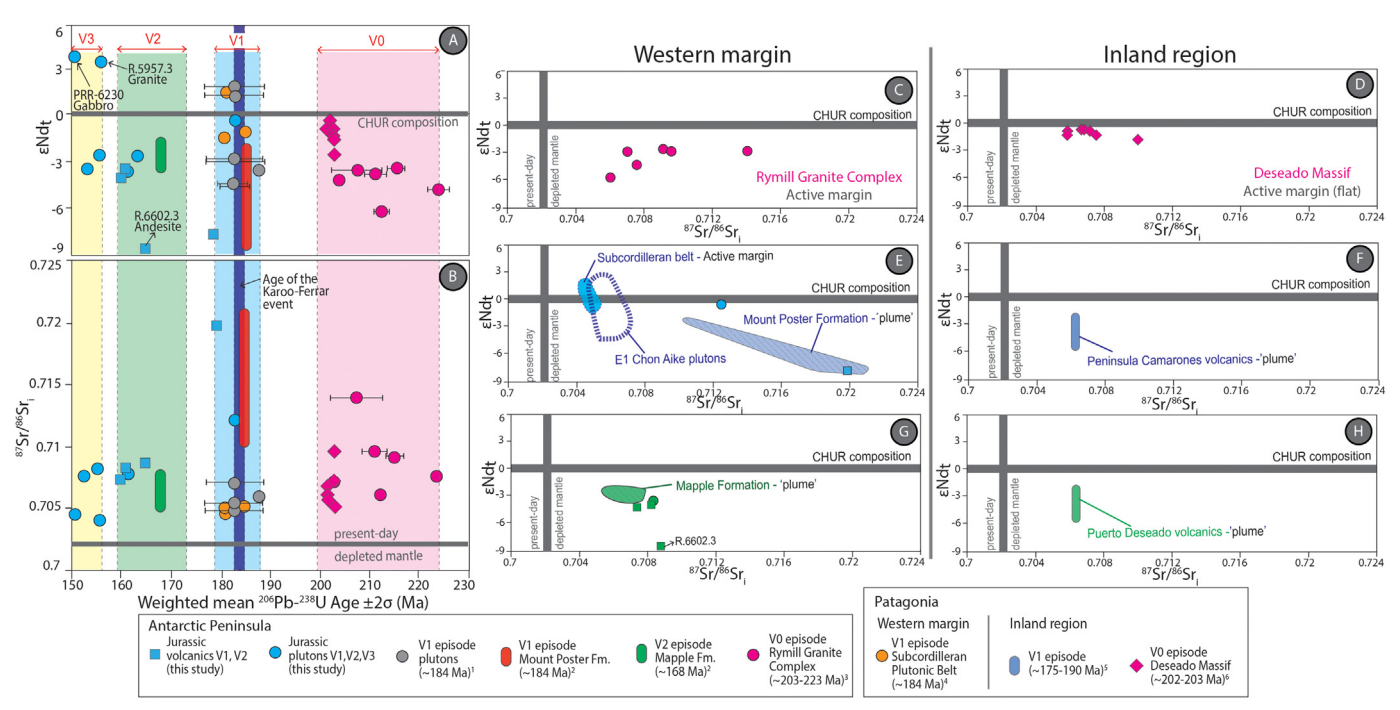


Fig. 4. (A, B) Temporal evolution of whole rock εNd_t (A) and ⁸⁷Sr/⁸⁶Sr_i (B) isotopic compositions of Late Triassic-Jurassic igneous rocks in Patagonia and the Antarctic Peninsula. Data are only reported from samples that are considered to yield accurate crystallisation ages. (C to H) Compilation of εNd_t and ⁸⁷Sr/⁸⁶Sr_i values shown in (A) and (B) for rock units of the Inland Region and the Western Margin. Data from V0 are presented in (C) and (D), V1 in (E) and (F) and V2 in (G) and (H). Data sources 1: Leat et al. (2009) and Riley et al. (2016); 2: Riley et al. (2001); 3: Bastias et al. (2019, 2020a); 4: Rapela et al. (2005); 5: Pankhurst and Rapela (1995); 6: Rapela and Pankhurst (1996). The detailed methodology and full dataset are presented in Bastias et al. (2021).

~2 and -9 (Fig. 4a), and ~0.721 and 0.705, respectively (Fig. 4b; Riley et al., 2001, 2016; Rapela et al., 2005; Leat et al., 2009). Furthermore, while the V1-aged units of the western margin yield ϵ Nd_i and ϵ Sr/86Sr_i values that range between 1.9 and ϵ 7.8, and 0.720 and 0.704, respectively (Leat et al., 2009; Riley et al., 2001, 2017), Pankhurst and Rapela (1995) reported bulk-rock isotopic compositions in the Inland Region, which yield ϵ Nd_i and ϵ Sr/86Sr_i values of ϵ 4 ± 2 and 0.707 ± 0.0003, respectively (Fig. 4a, b). A larger range in Nd and Sr isotopic compositions is recorded in V1-aged rocks when compared to episodes V0, V2 and V3 (Fig. 4a, b), suggesting they may be derived from more heterogeneous source regions, with a dominant crustal component, corroborating Riley et al. (2001).

Volcanic and plutonic rocks that crystallised during the V2 (~173–160 Ma) and V3 (~157–145 Ma) episodes yield similar ϵ Nd_i and ϵ Sr_isofsr_i compositions to V0-aged rocks, with values spanning between ~ 9 to -1 (ϵ Nd_i; Fig. 4a), and ~ 0.704 and 0.720 (ϵ Sr_isofsr_i; Fig. 4b; Riley et al., 2001). Exceptions are syenogranites R.5957.3 (V2; 156 \pm 1 Ma) and PRR-6230 (V3; 151 \pm 1 Ma), and andesite R.6602.3 (V2; 165 \pm 1 Ma) from the Antarctic Peninsula, which yield either significantly higher (>3; PRR-6230 and R.5957.3; Fig. 4a) or lower (<-9; R6602.3; Fig. 4g) ϵ Nd_i values. We consider these rocks to record anomalous magmatism, which is discussed in the following section. The plutonic and volcanic rocks of the V0 and V2 episodes yield small variations in their whole rock Nd and Sr isotopic compositions compared to V1 and V3-aged rocks (Fig. 4 a, b). A comparison of crystallisation age with isotopic composition reveals no distinct trend, although the most juvenile rocks formed during the V3 episode (Fig. 4a, b).

4.4. Hf isotopes in zircon

A comparison of in-situ zircon ϵ Hf_t compositions and crystallisation age (zircon 206 Pb— 238 U) of plutonic and volcanic rocks of the Antarctic Peninsula is presented in Fig. 5. This dataset combines our new data, which spans the V1, V2 and V3 episodes within the Antarctic Peninsula,

with data from the Triassic Rymill Granite Complex (V0; Antarctic Peninsula; Bastias et al., 2020). Triassic zircons yield ϵ Hf_t compositions that are less radiogenic than CHUR with values ranging between ~0 and -10. With the exception of rhyolite R.6871.3 and granite R.5957.3, most of the Jurassic zircons yielded ϵ Hf_t values between ~0 and -5. Granite R.5957.3 yields an elevated ϵ Hf_t value of >5, while rhyolite R.6871.3 yields a relatively unradiogenic value of <-8 (Fig. 5).

5. Discussion

5.1. The tectonic history of Patagonia and the Antarctic Peninsula between ~223 and ~ 145 Ma: An active margin origin for the Chon Aike magmatic province

A combination of the geochemical and isotopic compositions of the Jurassic igneous rocks exposed along the Western Margin and in the Inland Region suggests they all formed in a continental arc setting (Figs. 3-5). This conclusion modifies previous interpretations (e.g. Bryan et al., 2002; Pankhurst et al., 2000; Riley et al., 2001; Storey et al., 1992) that suggested the early deposits of the Chon Aike magmatic province in eastern and central Patagonia formed by the coupled action of an active margin and the peripheral thermal effect of the Karoo mantle plume. A supra-subduction zone origin is supported by: (i) enriched LILE and LREE, with negative Nb, Ta, Sr and Ti anomalies (Fig. 3d, e) in all of the Jurassic igneous rocks, which are typical of slab-dehydration reactions and thus active margins, (ii) the trace element compositions of Jurassic igneous rocks in the Inland Region (eastern and central Patagonia) and the Western Margin (Patagonia and the Antarctic Peninsula; Figs. 3d, e) are indistinguishable, and thus it is likely that they evolved via the same magmatic processes, and (iii) the whole rock Nd and Sr, and zircon Hf isotopic compositions of Late Triassic-Jurassic igneous rocks (Figs. 4, 5) show that the magmas formed from mixed sources that resided within the continental crust. Therefore, unlike the igneous units of the Karoo and Ferrar LIPs, the involvement of

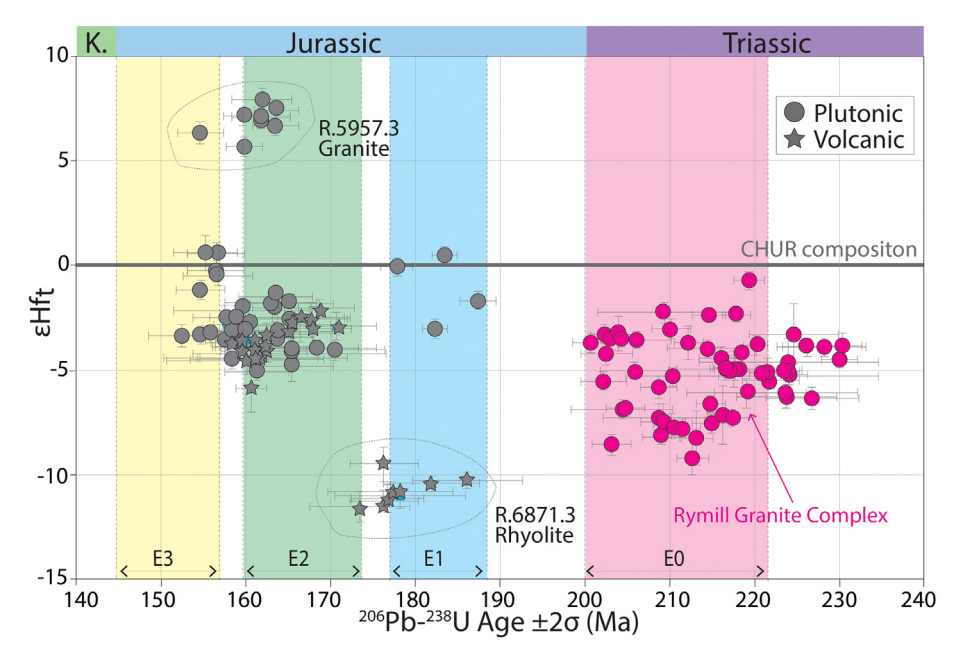


Fig. 5. Selected zircon $^{206}U-^{238}Pb$ concordia ages and ϵHf_t values from volcanic and plutonic rocks of the Antarctic Peninsula during the Late Triassic-Jurassic period. Data are from this study (Jurassic) and Bastias et al. (2020). Each data point corresponds to a pair of ablations collected in a single zircon crystal. All $^{206}U-^{238}Pb$ uncertainties are quoted at $\pm 2\sigma$. The detailed dataset is presented in Bastias et al. (2021).

a mantle plume is not necessary to generate any of the chronological, geochemical or isotopic characteristics of the Chon Aike magmatic province. Here we present a revised geological evolution for the Late Triassic-Jurassic in Patagonia and the Antarctic Peninsula.

5.1.1. V0 episode: ~223-200 Ma

Active margin magmatism commenced as early as ~223 Ma, forming the Rymill Granite Complex in the Antarctic Peninsula (Bastias et al., 2020; Riley et al., 2020b) and Late Triassic magmatism in the Deseado Massif in eastern Patagonia (Navarrete et al., 2019; Pankhurst et al., 1993). The location of the Deseado Massif within eastern Patagonia would have been at least ~1100-1000 km distant from the palaeotrench, suggesting these magmas formed above a low angle slab (the South Gondwanian flat-slab of Navarrete et al., 2019). The presence of a flattened slab is supported by a Late Triassic-Early Jurassic contractional metamorphic phase that is recorded in the southwestern Patagonian fore-arc (Chonide Orogeny; e.g. Thomson and Hervé, 2002; Sepúlveda et al., 2008; Willner et al., 2009; Fig. 6a). However, Late Triassic arc plutons are exposed along the Antarctic Peninsula (Rymill Granite Complex; e.g. Pankhurst, 1982; Wever et al., 1994; Leat and Scarrow, 1995; Flowerdew et al., 2006; Bastias et al., 2020), proximal to the palaeotrench, implying that any flattened slab must have been spatially restricted to present-day southern Patagonia and the northern Antarctic Peninsula (Fig. 6a). Interestingly, this is entirely consistent with several paleogeographic reconstructions that juxtapose the northern Antarctic Peninsula and southern Patagonia during the Late Triassic-Middle Jurassic (e.g. Lawver et al., 1998; Ghidella et al., 2002; Jokat et al., 2003; Fig. 6a).

5.1.2. Magmatic quiescence: ~200-188 Ma

Magmatism is not recorded within Patagonia or the Antarctic Peninsula during the interval ~ 200–188 Ma. Coeval magmatic quiescence has been proposed for central Chile and the Neuquen Basin in Argentina (e.g. Howell et al., 2005; Oliveros et al., 2019), revealing a paucity or lack of magmatism along a potential trench parallel distance of ~5000 km (see also the publications of Mišković et al., 2009 and Spikings et al., 2015). Some studies equate this magmatic gap with a

lack of active subduction to the south of ~18°S within South America during the Early Jurassic (e.g. Mpodozis and Ramos, 2008).

5.1.3. V1 episode: ~188-178 Ma

Arc-related magmatism resumed at ~188 Ma (Fig. 3d, e) along the western margin of northern Patagonia, the southern Antarctic Peninsula and in eastern Patagonia (Figs. 2, 6b). The igneous rocks in eastern Patagonia have been grouped into the V1 Chon Aike episode (e.g. Pankhurst et al., 2000), and were interpreted by Riley et al. (2001) as melts of subduction-modified lower crust, where melting was triggered by extension associated with the break-up of Gondwana, with peripheral heating from the Karoo mantle plume (Riley et al., 2001). However, the compiled and new data do not require the existence of heat derived from a mantle plume, and the simplest explanation of the geochemical and isotopic compositions data, combined with geographic distribution. is that these magmas formed above a flattened-slab, implying a resumption of flat-slab subduction, which would be consistent with their geochemical and isotopic compositions and geographic location (Fig. 6b). The whole rock Nd-Sr and zircon Hf isotopic compositions of the rocks that formed during the V1 episode (Fig. 4a, b) reveal a dominance of crustal sources, partially corroborating the model of Riley et al. (2001, 2017). The V1-aged flat-slab may have either been a reactivated section of the Triassic flat-slab (Fig. 6a), or it may correspond to younger and buoyant oceanic lithosphere that was subducted beneath Gondwana towards the end of magmatic quiescence between ~200-188 Ma. Nevertheless, the nature of the subducted oceanic lithosphere that resumed the subduction during the V1 episode remain unknown.

5.1.4. V2 episode: ~173-160 Ma

The V2 magmatic episode occurred during the interval ~ 173–160 Ma, and is exposed along the western margin of southern Patagonia, the Deseado Massif in eastern Patagonia and the northeastern Antarctic Peninsula (Figs. 2a, b). The period was temporally separated from the older V1 episode (~188–178 Ma) by an apparent magmatic gap during ~178–173 Ma, although a few zircon grains yield ²⁰⁶Pb—²³⁸U concordia ages that span this gap (Fig. 5). The magmas produced during the V2 episode yield trace element compositions that are similar to those that formed during the V0 and V1 episodes (Figs. 3d, e), suggesting a

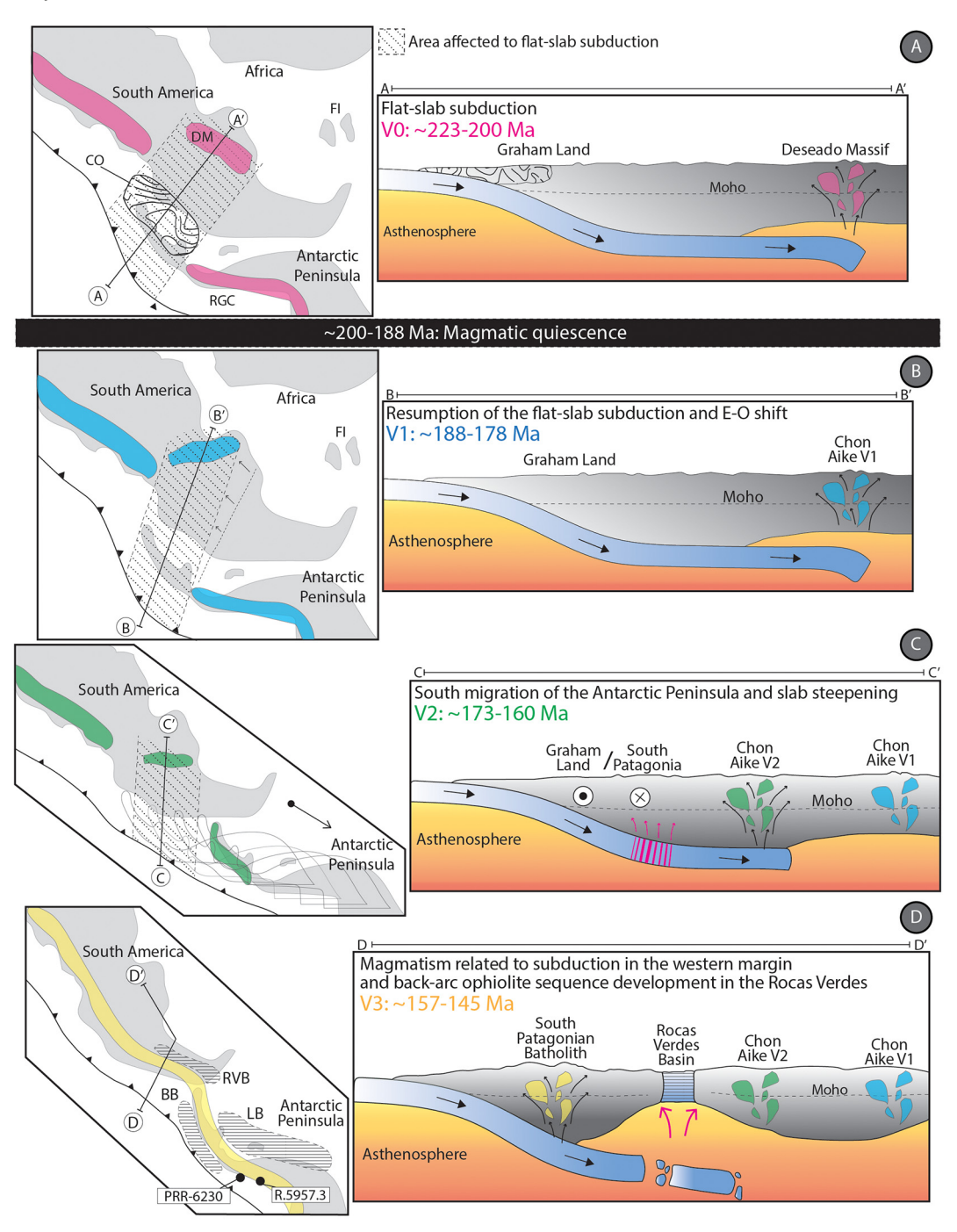


Fig. 6. Schematic paleo-reconstruction of southwestern Gondwana for the Late Triassic-Jurassic. (A) V0: ~223–200 Ma, initiation of flat-slab subduction and active margin magmatism in the Deseado Massif (DM), along with metamorphism associated with the Chonide Orogeny (CO; e.g. Thomson and Hervé, 2002). The geographic extent of the flat-slab is limited to the south by the arc rocks of the Rymill Granite Complex (Bastias et al., 2020). Fl: Falkland Islands. (B) V1: ~189–178 Ma, following magmatic quiescence during ~200–188 Ma, the active margin resumed forming arc rocks in the southern Antarctic Peninsula and in Patagonia. (C) V2: ~173–160 Ma, migration of the arc axis towards the north of the Antarctic Peninsula, and trenchward within Patagonia. The Antarctic Peninsula drifted southward with respectively to Patagonia, which is shown as a series of outlines of the Antarctic Peninsula in gray. (D) V3: ~157–145 Ma, emplacement of the arc along the West Margin of the Antarctic Peninsula and Patagonia. Back-arc extension formed oceanic lithosphere in the Rocas Verdes Basin (RVB; Calderón et al., 2007). Coeval deep-marine sedimentary rocks were deposited in the fore-arc and back-arc of the Antarctic Peninsula, which corresponds to the Byers Basin (BB; Bastias et al., 2019) and the Larsen Basin (LB; Hathway, 2000), respectively.

continuation of active margin magmatism. The whole rock Sr—Nd isotopic compositions of the V2 episode yield a smaller range than during V1 (Fig. 5), although they are not significantly different to the rocks that formed during the Late Triassic (episode V0). The presence of coeval arc magmas in the northern Antarctic Peninsula (Fig. 2b) and eastern Patagonia (Fig. 2a) implies a continuation of apparently persistent flatslab subduction during ~173–160 Ma in Patagonia (Fig. 6c). The V2

episode within Patagonia is exposed to the southwest of the V1 rocks (~188–178 Ma), although they are both attributed to flat-slab magmatism (Figs. 2b, c). We consider this to be a result of modification of the slab architecture (Fig. 6c), perhaps via either slab failure or slab steepening. This complement previous authors (e.g. Bryan et al., 2002; Riley et al., 2001) suggesting that the migration of the volcanism was partially generated by the action of the active margin. The presence

of V2-aged arc magmas in the northern Antarctic Peninsula (~173–160 Ma, Fig. 2b), which were coeval with those in eastern Patagonia (Deseado Massif; Fig. 2a), suggests that the Antarctic Peninsula may have migrated south relative to Patagonia during ~180–170 Ma (Fig. 6c), which is consistent with several reconstructions (e.g. Ghidella et al., 2002; Grunow, 1993; Hervé et al., 2006; Lawver et al., 1998). A lack of evidence for rifting between Patagonia and the Antarctic Peninsula during the V2 time (~173–160 Ma) suggests that this transcurrent sinistral displacement did not significantly extend the crust. Sinistral displacement during the Middle or Late Jurassic was also suggested by Hervé et al. (2006), to account for similarities and differences in the Mesozoic sedimentary rocks of western Patagonia and the northern Antarctic.

5.1.5. V3 episode: ~157-145 Ma

Magmatism during the V3 episode is recorded along the western margin of Patagonia and the Antarctic Peninsula (Fig. 2a, b). Previous authors interpreted this period as a transition from mantle-plume related to active margin magmatism (e.g. Hervé et al., 2007; Pankhurst et al., 2000). Most of the rocks that formed during the V3 episode in Patagonia are located within the South Patagonian Batholith (Hervé et al., 2007), and minor exposures are found in central Patagonia (Fig. 2a). With a few exemptions in the southern Antarctic Peninsula (Fig. 2b), V3-aged magmatism is mostly constrained to the north of the Antarctic Peninsula and has a similar geographic distribution to rocks of the V2 episode (Fig. 2b). Whole rock geochemistry (Figs. 3d, e) and isotopic tracing (Figs. 4a, b) suggest these magmas formed above an active margin, and thus it is likely they formed above the same subducted slab that gave rise to the older Jurassic and Triassic igneous rocks (Pankhurst et al., 2000). Importantly, there are no clear geochemical differences between the V3-aged, and older Jurassic and Triassic igneous rocks. Whole rock (Sr—Nd) and zircon (Hf) isotopic data from four rocks suggest that the source regions for V3 magmatism were similar, or perhaps the same as those for the earlier V0-V2 periods (~223-160 Ma), albeit with a higher proportion of a juvenile component. Granite R.5957.3 (V3 episode, ~156 Ma) and gabbro PRR-6230 (V3 episode, ~151 Ma) yield the most juvenile Sr-Nd whole rock compositions (Fig. 4), which are consistent with zircon EHft values that range between 8 and 5 (Fig. 4; granite R.5957.3). We propose that these rocks were located at the boundaries of the postulated flat-slab (Fig. 6d), and thus they could have been influenced by asthenospheric upwelling through a slab window, inducing greater amounts of melting of isotopically juvenile man-

Progressive western migration of V1- and V2-aged magmatism (Figs. 6b, c) ceased during the V3 episode, by which time a majority of magmatism was focused along the Western Margin (Fig. 6d). Trenchward migration of magmatism from the Inland Region in Patagonia was most likely caused by gradual steepening of the flat-slab during ~188–160 Ma. Back-arc extension during V3 time lead to the formation of oceanic lithosphere in the Rocas Verdes Basin (Fig. 6d; Stern and de Wit, 2003; Calderón et al., 2007), which is exposed along southwestern Patagonia (Stern and de Wit, 2003). The basement of the Rocas Verdes Basin is composed of pillow lavas, dykes and gabbros that have been interpreted as part of an ophiolite sequence that formed along a midocean-ridge (Stern and de Wit, 2003). The prime cause of an increased flux of mantle-derived material in the Rocas Verdes Basin may be related to decompression associated with crustal thinning, although its relationship, if any, to modifications of the slab architecture (e.g. steepening) are unclear (Fig. 6d).

5.2. Implications for the formation of the Rocas Verdes Basin and the opening of the Weddell Sea

The Weddell Sea is located to the east of the Antarctic Peninsula (Fig. 2b), and its Jurassic-Cretaceous formation (e.g. König and Jokat, 2006) lead to the opening of the south Atlantic and the separation of

the South American, African and Antarctic plates (Fig. 7). The initial extent and paleopositions of the crustal blocks that formed Gondwana are still debated (e.g. Elliot, 1992; Lawver et al., 1998; Verard et al., 2012), although there is a general consensus that the earliest oceanic lithosphere in the Weddell Sea formed during ~160-145 Ma (e.g. Ghidella et al., 2002; König and Jokat, 2006; Lawver et al., 1998; Riley et al., 2020a). This period coincides with V3-aged magmatism along the Western Margin of Patagonia (~157–145 Ma), and within the Rocas Verdes Basin (Fig. 6d, 7; e.g. Dalziel, 1981), which started rifting during ~152–142 Ma (Calderón et al., 2007). These coeval events perhaps reveal common causes for the formation of oceanic lithosphere in the back-arc Rocas Verdes Basin and the opening of the Weddell Sea. Mafic crust of the basement of the Rocas Verdes Basin strikes parallel to the western margin of Patagonia, whereas the earliest oceanic lithosphere of the Weddell Sea had a sub east-west orientation according to numerous paleo-geographic reconstructions of the Weddell Sea (e.g. Ghidella et al., 2002; König and Jokat, 2006). Therefore, we speculate that V3-aged oceanic lithosphere in southern Patagonia, and along the present boundaries of the northern Antarctic Peninsula formed at a triple plate junction (Fig. 7). In this scenario, the Weddell Sea would represent a fully rifted, successful arm of the triple junction that generated oceanic lithosphere until ~33 Ma (e.g. Ghidella et al., 2002), while the Rocas Verdes Basin formed oceanic lithosphere during the Late Jurassic, but stalled during Cretaceous basin inversion events. No clear

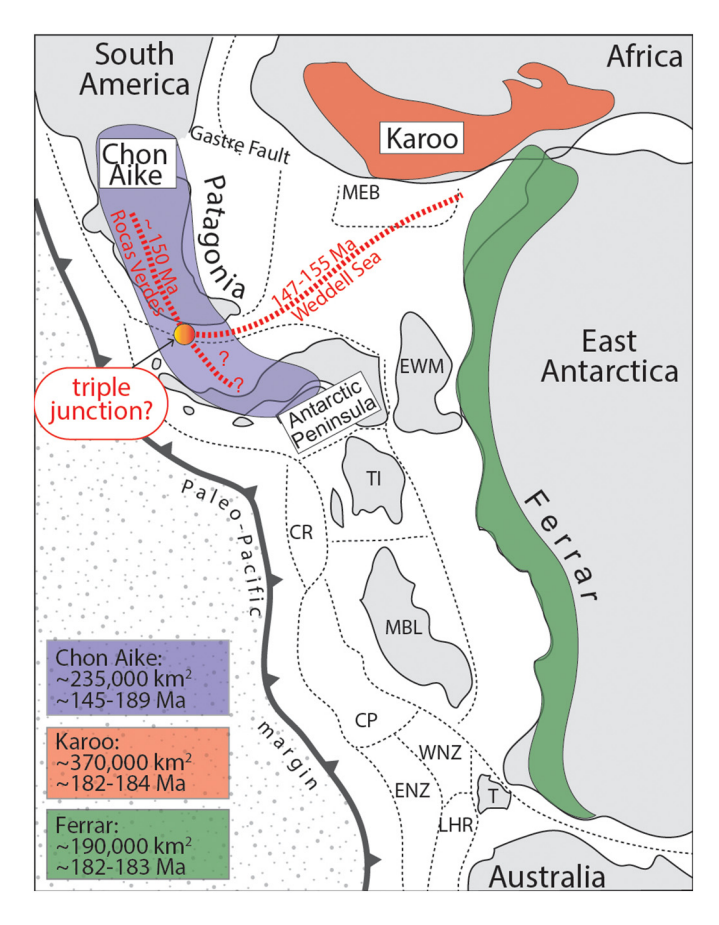


Fig. 7. Reconstruction of Gondwana during the Jurassic (after Grunow, 1993, Elliot and Fleming, 2000, and Jordan et al., 2017) illustrating the schematic distribution of the Karoo and Ferrar LIPs, and the Chon Aike magmatic province. The coeval opening of the Weddell Sea and the formation of ophiolite sequences in the Rocas Verdes Basin suggests the potential presence of a triple junction located in southern Patagonia or to the north of the Antarctic Peninsula. CR: Chatham Rise, TI: Thurston Island, EWM: Ellsworth-Whitmore Mountains, MBL: Marie Byrd Land, CP: Campbell Plateau, WNZ: West New Zealand, ENZ: East New Zealand, LHR: Lord Howe Rise, T: Tasmania, MEB: Maurice Ewing Bank.

evidence is known for the third arm of this suspect triple junction, although we predict that it may have influenced the Antarctic Peninsula.

5.3. Implications for the Karoo-Ferrar event and the Early Jurassic environmental crisis

The Karoo-Ferrar event has been traditionally considered to include the Karoo and Ferrar LIPs, and the V1 episode of the Chon Aike magmatic province (e.g. Storey et al., 2013; Sensarma et al., 2017), given the contemporaneity and spatial juxtaposition of these units. This Early Jurassic event represents one of the most voluminous Phanerozoic magmatic episodes (e.g. Riley and Knight, 2001; Storey et al., 2013; Sensarma et al., 2017), and it has been proposed as the leading explanation for environmental changes that triggered the Toarcian-Pleinsbachian Oceanic Anoxic Event, which in turn drove multi-phase mass extinction (e.g. Caruthers et al., 2014). Several authors have suggested that these igneous rocks formed as a consequence of mantle plume activity that accompanied the onset of the break-up of southwestern Gondwana (e.g. Storey et al., 2013). However, our new data and compilation show that the Chon Aike magmatic province can be accounted for entirely by active margin processes. This significantly impacts estimates of the volume of magma produced by Early Jurassic plume-related magmatism. The total volumes of the magmatic products emplaced by the Karoo and Ferrar LIPs are ~370,000 km³ (Svensen et al., 2012) and ~190,000 km³ (Elliot and Fleming, 2000; Storey et al., 2013), respectively, while the Chon Aike magmatic province has an estimated volume of ~235,000 km3 (Pankhurst et al., 1998; Storey et al., 2013), representing up to ~30% of the Karoo-Ferrar event. Therefore, the extent of the Karoo-Ferrar event should be revised with the exclusion of the Chon Aike magmatic province, and thus the causes of rapid Jurassic environmental changes may need to be reassessed.

The original sensu stricto use of the term LIP refers to a group of mafic igneous rocks that were emplaced within a few million years and with exposures covering an area of at least 100,000 km² (e.g. Coffin and Eldholm, 1992). Although this terminology has been revised with the introduction of felsic members (e.g. Bryan et al., 2002), there are significant uncertainties about the volume of the V1, V2 and V3 episodes of the Chon Aike magmatic province. In addition, the Chon Aike magmatic province lacks a high-precision geochronological framework, which is required to accurately constrain the duration of a short igneous event (e.g. Karoo LIP, Svensen et al., 2012; Sell and Ovtcharova, 2014; Ferrar, Burgess et al., 2015; Greber et al., 2020). Therefore, we suggest that further work is required to determine the timing and volume of magmatism that is associated with the Chon Aike magmatic province in Patagonia and the Antarctic Peninsula.

6. Conclusions

A combination of the geochemical and isotopic compositions of the Late Triassic to Jurassic volcanic and plutonic rocks (~223-145 Ma) exposed along the Western Margin and in the Inland Region of the Antarctic Peninsula and Patagonia suggests they formed in a continental arc setting. This conclusion argues against the necessity to invoke the involvement of the Karoo mantle plume in the formation of the Chon Aike magmatic province, and supports previous interpretations that suggest it formed via Jurassic active margin magmatism along Patagonia and the Antarctic Peninsula. A supra-subduction zone origin is supported by (i) enriched LILE and LREE, with negative Nb, Ta and Ti anomalies, which are typical of slab-dehydration reactions and thus active margins, (ii) indistinguishable major oxide and trace element compositions of Late Triassic and Jurassic igneous rocks in both the Inland Region (eastern and central Patagonia) and the Western Margin (Patagonia and the Antarctic Peninsula), and (iii) whole rock Nd and Sr, and zircon Hf isotopic compositions of Late Triassic-Jurassic igneous rocks that reveal mixed sources that resided within the continental crust. We argue against the hypothesis that these rocks formed by the same mechanisms that created the Karoo and Ferrar LIPs. We suggest that the extent of the Karoo-Ferrar event should be revised, and the Chon Aike magmatic province should be excluded from this province, and thus the causes of rapid Early Jurassic environmental change should be reassessed.

The spatial distribution of arc magmas suggests a subducted flat slab segment existed since at least ~223–200 Ma, and formed a broad spatial geographic spread of active margin magmatism within Patagonia, which gradually migrated towards the trench, via slab steepening, reaching a normal trench-arc distance at ~157–145 Ma. The attainment of a normal trench-arc distance temporally coincided with rifting that formed oceanic lithosphere of the Weddell Sea, and back-arc basin extension of the Rocas Verdes Basin, possibly revealing a causal relationship between these processes. We speculate that the two rift axes may have originated from a triple junction that was located between southern Patagonia and the northern Antarctic Peninsula, and lead to the disassembly of southern Gondwana.

Declaration of Competing Interest

The authors declare that they have no known competing financial interests or personal relationships that could have appeared to influence the work reported in this paper.

Acknowledgements

The authors are grateful for the extensive logistical support provided by the Instituto Antártico Chileno (INACH) during two field campaigns to the Antarctic Peninsula. This manuscript is based on rocks provided by the British Antarctic Survey and the Polar Rock Repository with support from the National Science Foundation, under Cooperative Agreement OPP-1643713. Support was provided by the staff and laboratories of the Isotope Geochemistry Group of the University of Geneva. This Project was funded by the Chilean Antarctic Institute Project RT-06-14 and the University of Geneva. J.B. holds a PhD-scholarship from CONICYT-Chile.

References

Bastias, J., 2020. The Triassic–Cretaceous Tectonomagmatic History of the Antarctic Peninsula constrained by Geochronology, Thermochronology and Isotope Geochemistry. Université de Genève Thèse. 2020b. 10.13097/archive-ouverte/unige:143280 https://archive-ouverte.unige.ch/unige:143280.

Bastias, J., Fuentes, F., Aguirre, L., Hervé, F., Demant, A., Deckart, K., Torres, T., 2016. Very low-grade secondary minerals as indicators of palaeo-hydrothermal systems in the Upper Cretaceous volcanic succession of Hannah Point, Livingston Island, Antarctica. Appl. Clay Sci. 134, 246–256. https://doi.org/10.1016/j.clay.2016.07.025.

Bastias, J., Calderon, M., Israel, L., Herve, F., Spikings, R., Pankhurst, R., Castillo, P., Fanning, M., Ugalde, R., 2019. The Byers Basin: Jurassic-Cretaceous tectonic and depositional evolution of the forearc deposits of the South Shetland Islands and its implications for the northern Antarctic Peninsula. Int. Geol. Rev. https://doi.org/10.1080/00206814.2019.1655669.

Bastias, J., Spikings, R., Ulianov, A., Burton-Johnson, A., Chiaradia, M., Baumgartner, L., Hervé, F., Bouvier, A.S., 2020. The Gondwanan margin in West Antarctica: insights from Late Triassic magmatism of the Antarctic Peninsula. Gondwana Res. 81, 1–20. https://doi.org/10.1016/j.gr.2019.10.018.

Bastias, J., Spikings, R., Riley, T., Ulianov, A., Grunow, A., Chiaradia, M., Hervé, F., 2021. Data on the Arc Magmatism Developed in the Antarctic Peninsula and Patagonia During the Late Triassic – Jurassic: A Compilation of New and Previous Geochronology, Geochemistry and Isotopic Tracing Results (Data in Brief, In review).

Bouvier, A., Vervoort, J.D., Patchett, P.J., 2008. The Lu–Hf and Sm–Nd isotopic composition of CHUR: constraints from unequilibrated chondrites and implications for the bulk composition of terrestrial planets. Earth Planet. Sci. Lett. 273, 48–57.

Bryan, S.E., Riley, T.R., Jerram, D.A., Leat, P.T., Stephens, C.J., 2002. Silicic volcanism: an under-valued component of large igneous provinces and volcanic rifted margins. In: Menzies, M.A., Klemperer, S.L., Ebinger, C.J., Baker, J. (Eds.), Magmatic Rifted Margins. Geological Society of America Special Paper vol. 362, pp. 99–118.

Burgess, S.D., Bowring, S.A., Fleming, T.H., Elliot, D.H., 2015. High-precision geochronology links the Ferrar large igneous province with early-Jurassic Ocean anoxia and biotic crisis. Earth Planet. Sci. Lett. 415, 90–99.

Calderón, M., Fildani, A., Hervé, F., Fanning, C.M., Weislogel, A., Cordani, U., 2007. Late Jurassic bimodal magmatism in the northern sea-floor remnant of the Rocas Verdes Basin, southern Patagonian Andes. J. Geol. Soc. 164, 1011–1022 (London).

- Caruthers, A.H., Smith, P.L., Gröcke, D.R., 2014. The Pliensbachian–Toarcian (Early Jurassic) extinction: a North American perspective. Spec. Pap. Geol. Soc. Am. 505, pp. 225–243.
- Coffin, M.F., Eldholm, O., 1992. Volcanism and continental break-up: a global compilation of large igneous provinces. In: Storey, B.C., Alabaster, T., Pankhurst, R.J. (Eds.), Magmatism and the Causes of Continental Break-up: Geological Society [London] Special Publication. 68, pp. 17–30.
- Coltice, N., Phillips, B.R., Bertrand, H., Ricard, Y., Rey, P., 2007. Global warming of the mantle at the origin of flood basalts over supercontinents. Geology 35, 391–394.
- Cox, 1988. The Karoo province. In: Macdouoall, J.D. (Ed.), Continental Flood Basalts. Kluwer Academic Publishers, Dordrecht, pp. 239–327.
- Cox, K.G., 1992. Karoo igneous activity, and the early stages of the break-up of Gondwanaland. Spec. Publ. Geol. Soc. Lond. 68, 137–148.
- Dalziel, I.W.D., 1981. Back-arc extension in the southern Andes: A review and critical reappraisal. Royal Society of London Philosophical Transactions. Series A 300, 319–355.
- Dalziel, I., Lawver, L., Murphy, J., 2000. Plumes, orogénesis, and supercontinental fragmentation. Earth Planet. Sci. Lett. 178, 1–11.
- De La Roche, H., Leterrier, J., Grandclaude, P., Marchal, M., 1980. A classification of volcanic and plutonic rocks using R1R2-diagram and major-element analyses its relationships with current nomenclature. Chem. Geol. 29, 183–210.
- Duncan, R.A., Richards, M.A., 1991. Hotspots, mantle plumes, flood basalts and true polar wander. Rev. Geophys. 29, 31–50.
- Elkins-Tanton, L.T., 2005. Continental magmatism caused by lithospheric delamination. In: Foulger, R., Natland, J.H., Presnall, D.C., Anderson, D.L. (Eds.), Plates, Plumes and Paradigms. vol. 388. Geological Society of America, Special Publications, pp. 449–461.
- Elliot, D.H., 1992. Jurassic magmatism and tectonism associated with Gondwanaland break-up: an Antarctic perspective. In: Storey, B.C., Alabaster, T., Pankhurst, R.J. (Eds.), Magmatism and the causes of continental breakup: Geological Society [London] Special Publication. 68, pp. 165–184.
- Elliot, D.H., Fleming, T., 2000. Weddell triple junction: the principal focus of Ferrar and Karoo magmatism during initial breakup of Gondwana. Geology 28, 539–542.
- Elliot, D.H., Fleming, T.H., 2004. Occurrence and dispersal of magmas in the Jurassic Ferrar large igneous province, Antarctica. Gondw. Res. 7 (1), 223–237.
- Encarnacion, J., Fleming, T.H., Elliot, D., Eales, H.V., 1996. Synchronous emplacement of Ferrar and Karoo dolerites and the early breakup of Gondwana. Geology 24, 535–538.
- Fanning, C.M., Laudon, A., T. S., 1997. Mesozoic volcanism and sedimentation in eastern Ellsworth Land, West Antarctica; conflicting evidence for arc migration? Geol. Soc. Am. Progr. Abstr. 29, A51517.
- Féraud, G., Alric, V., Fornari, M., Bertrand, H., Haller, M., 1999. 40Ar/39Ar dating of the Jurassic volcanic province of Patagonia: migrating magmatism related to Gondwana break-up and subduction. Earth Planet. Sci. Lett. 172, 83–96.
- Flowerdew, M.J., Millar, I.L., Vaughan, A.P.M., Horstwood, M.S.A., Fanning, C.M., 2006. The source of granitic gneisses and migmatites in the Antarctic Peninsula: a combined U-Pb SHRIMP and laser ablation Hf isotope study of complex zircons. Contrib. Mineral. Petrol. 151, 751–768.
- Ghidella, M.E., Yáñez, G., LaBrecque, J.L., 2002. Revised tectonic implications for the magnetic anomalies of the western Weddell Sea. Tectonophysics 347, 65–86.
- Greber, N.D., Davies, J.H., Gaynor, S., Jourdan, F., Bertrand, H., Schaltegger, U., 2020. New high precision U-Pb ages and Hf isotope data from the Karoo large igneous province; implications for pulsed magmatism and early Toarcian environmental perturbations. Results Geochem., 100005. https://doi.org/10.1016/j.ringeo.2020.100005.
- Grunow, A.M., 1993. Creation and destruction of Weddell Sea floor in the Jurassic. Geology 21, 647–650.
- Hathway, B., 2000. Continental rift to back-arc basin: Jurassic- Cretaceous stratigraphical and structural evolution of the Larsen Basin, Antarctic Peninsula. J. Geol. Soc. Lond. 157, 417–432. https://doi.org/10.1144/jgs.157.2.417.
- Hawkesworth, C., Kelly, S., Turner, S., le Roux, A., 1999. Mantle processes during Gondwana break-up and dispersal. J. Afr. Earth Sci. 28, 239–261.
- Hervé, F., Miller, H., Pimpirev, C., 2006. Patagonia-Antarctic connections before Gondwana break-up. In: Futterer, D., et al. (Eds.), Antarctica: Contributions to Global Earth Sciences. Springer, Berlin, pp. 217–228.
- Hervé, F., Pankhurst, R., Fanning, M., Calderón, M., Yaxley, G., 2007. The south Patagonian batholith: 150 my of granite magmatism on a plate margina. Lithos 97, 373–394.
- Howell, J.A., Schwarz, E., Spalletti, L., Veiga, G.D., 2005. The Neuquén Basin: an overview. In: Veiga, G., et al. (Eds.), The Neuquén Basin: A Case Study in Sequence Stratigraphy and Basin Dynamics: The Geological Society, Special Publication. 252, pp. 1–14.
- Jokat, W., Boebel, T., König, M., Meyer, U., 2003. Timing and geometry of early Gondwana breakup. J. Geophys. Res. 108. https://doi.org/10.1029/2002JB001802.
- Jordan, T.A., Ferraccioli, F., Leat, P.T., 2017. New geophysical compilations link crustal block motion to Jurassic extension and strike-slip faulting in the Weddell Sea Rift System of West Antarctica. Gondw. Res. 42, 29–48.
- König, M., Jokat, W., 2006. The Mesozoic breakup of the Weddell Sea. J. Geophys. Res. 111, B12102.
- Lawver, L.A., Dalziel, I.W.D., Gahagan, L.M., 1998. A tight fit Early Mesozoic Gondwana, a plate reconstruction perspective. Mem. Nation Inst. Polar Res. Spec. Issue 53, 214–229
- Leat, P.T., Scarrow, J.H., Millar, I.L., 1995. On the Antarctic Peninsula batholith. Geol. Mag. 132, 399–4127.
- Leat, P.T., Flowerdew, M.J., Riley, T.R., Whitehouse, M.J., Scarrow, J.H., Millar, I.L., 2009. Zircon U–Pb dating of Mesozoic volcanic and tectonic events in Northwest Palmer Land and Southeast Graham Land, Antarctica. Antarct. Sci. 21, 633–641.
- Lovecchio, J.P., Naipauer, M., Cayo, L.E., Rohais, S., Giunta, D., Flores, G., Gerster, R., Bolatti, N.D., Joseph, P., Valencia, V.A., Ramos, V.A., 2019. Rifting evolution of the Malvinas basin, offshore Argentina: new constrains from zircon U/Pb geochronology and seismic characterization. J. South Am. Earth Sci. 95, 102253.

- Millar, I.L., Pankhurst, R.J., Fanning, C.M., 2002. Basement chronology of the Antarctic Peninsula: recurrent magmatism and anatexis in the Palaeozoic Gondwana margin. J. Geol. Soc. Lond. 159, 145–157.
- Miyashiro, A., 1978. Nature of alkalic volcanic rock series. Contrib Mineral Petrol 66, 91–104
- Mišković, A., Spikings, R.A., Chew, D.M., Kosler, J., Ulianov, A., Schaltegger, U., 2009. Tectonomagmatic evolution of Western Amazonia: geochemical characterization and zircon U–Pb geochronologic constraints from the Peruvian Eastern Cordilleran granitoids. Geol. Soc. Am. Bull. 121, 1298–1324.
- Mpodozis, C., Ramos, V., 2008. Tectónica jurásica en Argentina y Chile: Extensión, subducción oblicua, rifting, deriva y colisiones? Rev. Asoc. Geol. Argentina 63 (4), 481e497.
- Mukasa, S.B., Dalziel, I.W.D., 1996. Southernmost Andes and South Georgia island, north Scotia Ridge: zircon U–Pb and muscovite Ar/Ar age constraints on tectonic evolution of southwestern Gondwanaland. J. South Am. Earth Sci. 9, 349–365.
- Navarrete, C., Gianni, G., Encinas, A., Márquez, M., Kamerbeek, Y., Valle, N., Folguera, A., 2019. Upper Triassic to Middle Jurassic geodynamic evolution of southwestern Gondwana: from a large flat-slab to a mantle plume suction in a rollback subduction setting. Earth Sci. Rev. 194, 125–159. https://doi.org/10.1016/j.earscirev.2019. 05.002.
- Oliveros, V., Vasquez, P., Creixell, C., Lucassen, F., Ducea, M.N., Ciocca, I., Gonzalez, J., Espinoza, M., Salazar, E., Coloma, F., Kaseman, S., 2019. Lithospheric evolution of the Pre- and Early Andean convergent margin, Chile. Gondw. Res. 80, 202–227.
- Pankhurst, R.J., 1982. Rb-Sr geochronology of Graham Land. J. Geol. Soc. Lond. 139, 701–711
- Pankhurst, R.J., Rapela, C.R., 1995. Production of Jurassic rhyolite by anatexis of the lower crust of Patagonia. Earth Planet. Sci. Lett. 134, 23–36.
- Pankhurst, R.J., Rapela, C., Caminos, R., Elambias, E., Parica, C., 1992. A revised age for the granites of the central Somuncura Batholith, north Patagonia Massif. J. S. Ant. Earth Sci. 5, 321–325.
- Pankhurst, R.J., Rapela, C., Marquez, M., 1993. Geocronologia y petrogenesis de los granitodes jurasicos del noreste del Macizo del Deseado, (abstract) Congreso Geologico Argentino y II Congreso de Exploracion de Hidrocarburos 4, 7, La Plata. pp. 134–141.
- Pankhurst, R.J., Leat, P.T., Suroga, P., Rapela, C.W., Márquez, M., Storey, B.C., Riley, T.R., 1998. The Chon-Aike silicic igneous province of Patagonia and related rocks in Antarctica: a silicic large igneous province. J. Volcanol. Geotherm. Res. 81, 113–136.
- Pankhurst, R.J., Riley, T.R., Fanning, C.M., Kelley, S.P., 2000. Episodic silicic volcanism in Patagonia and the Antarctic Peninsula: chronology of magmatism associated with the breakup of Gondwana. J. Petrol. 41, 603–625.
- Peccerillo, A., Taylor, S.R., 1976. Geochemistry of Eocene calc-alkaline volcanic rocks from the Kastamonu area, Northern TurkeyContrib. Mineral. Petrol. 58, 63–81.
- Rapela, C.W., Pankhurst, R.J., 1996. Monzonite Suites: the Innermost Cordilleran Plutonism of Patagonia. Trans. R. Soc. Edinburgh 87, 193–203.
- Rapela, C.W., Pankhurst, R.J., Fanning, C.M., Hervé, F., 2005. Pacific subduction coeval with the Karoo mantle plume: the Early Jurassic subcordilleran belt of northwestern Patagonia. In: Vaughan, A.P.M., Leat, P.T., Pankhurst, R.J. (Eds.), Terrane Processes at the Margins of Gondwana. Geological Society, London, Special Publications. 246, pp. 217–240.
- Rex, D.C., 1976. Geochronology in relation to the stratigraphy of the Antarctic Peninsula. Br. Antarctic Surv. Bull. 32, 55–61.
- Richards, M.A., Duncan, R.A., Courtillot, V.E., 1989. Flood basalts and hot-spot tracks: plume heads and tails. Science 246, 103–107.
- Riley, T.R., 2006. Overlap of Karoo and Ferrar Magma types in KwaZulu-Natal, South Africa. J. Petrol. 47, 541–566. https://doi.org/10.1093/petrology/egi085.
- Riley, T., Knight, K., 2001. Review of pre-break-up Gondwana magmatism. Antarct. Sci. 13, 99–110.
- Riley, T.R., Leat, P.T., Pankhurst, R.J., Harris, C., 2001. Origins of large-volume rhyolite volcanism in the Antarctic Peninsula and Patagonia by crustal melting. J. Petrol. 42, 1043–1065
- Riley, T.R., Flowerdew, M.J., Hunter, M.A., Whitehouse, M.J., 2010. Middle Jurassic rhyolite volcanism of eastern Graham Land, Antarctic Peninsula: age correlations and stratigraphic relationships. Geol. Mag. 147, 581–595. https://doi.org/10.1017/ S0016756809990720.
- Riley, T.R., Flowerdew, M.J., Whitehouse, M.J., 2012. Chrono- and lithostratigraphy of a Mesozoic-Tertiary fore- to intra-arc basin: Adelaide Island, Antarctic Peninsula. Geol. Mag. 149, 768–782.
- Riley, T., Flowerdew, M., Pankhurst, R., Curtis, M., Millar, I., Fanning, M., Whitehouse, M., 2016. J. Geol. Soc. Lond. https://doi.org/10.1144/jgs2016-053.
- Riley, T.R., Flowerdew, M.J., Pankhurst, R.J., Curtis, M.L., Millar, I.L., Fanning, C.M., Whitehouse, M.J., 2017. Early Jurassic magmatism on the Antarctic Peninsula and potential correlation with the Subcordilleran plutonic belt of Patagonia. J. Geol. Soc. Lond. 174 (2), 365–376. https://doi.org/10.1144/jgs2016-053.
- Riley, T.R., Jordan, T.A., Leat, P.T., Curtis, M.L., Millar, I.L., 2020a. Magmatism of the Weddell Sea rift system in Antarctica: implications for the age and mechanism of rifting and early stage Gondwana breakup. Gondw. Res. 79, 185–196.
- Riley, T.R., Flowerdew, M.J., Millar, I.L., Whitehouse, M.J., 2020b. Triassic magmatism and metamorphism in the Antarctic Peninsula: identifying the extent and timing of the Peninsula orogeny. J. South Am. Earth Sci. https://doi.org/10.1016/j.jsames.2020.102732.
- Sensarma, S., Storey, B.C., Vivek, P., 2017. MalviyaGeological Society, London. Special Publications 463, 1–16. https://doi.org/10.1144/SP463.11.
- Seitz, S., Putlitz, B., Baumgartner, L.P., Bouvier, A.-S., 2018. The role of crustal melting in the formation of rhyolites: constraints from SIMS oxygen isotope data (Chon Aike Province, Patagonia, Argentina). Am. Miner. 103, 2011–2027. https://doi.org/ 10.2138/am-2018-6520.

Sell, B., Ovtcharova, M., 2014. Evaluating the temporal link between the Karoo LIP and climatic-biologic events of the Toarcian Stage with high-precision U-Pb geochronology. Earth Planet. Sci. Lett. 408, 48–56.

- Sepúlveda, F.A., Hervé, F., Calderón, M., Lacassie, J.P., 2008. Petrological and geochemical characteristics of metamorphic and igneous units from the allochthonous Madre de Dios terrane, southern Chile. Gondwana Res. 13 (2), 238–249. https://doi.org/ 10.1016/j.gr.2007.06.004.
- Spikings, R., Cochrane, R., Villagomez, D., Van der Lelij, R., Vallejo, C., Winkler, W., Beate, B., 2015. The geological history of northwestern South America: from Pangaea to the early collision of the Caribbean large Igneous Province (290–75 Ma). Gondw. Res. 27, 95–139.
- Sun, S.S., McDonough, W.F., 1989. Chemical and isotopic systematics of oceanic basalts: implications for mantle composition and processes. In: Saunders, A.D., Norry, M.J. (Eds.), Magmatism in Ocean Basins. Geologogical Society of London Special Publication 42, 313–345.
- Stern, C.R., de Wit, M.J., 2003. Rocas Verdes ophiolites, southernmost South America: remnants of progressive stages of development on oceanic-type crust in a continental margin back-arc basin. In: Dilek, Y., Robinson, P.T. (Eds.), Ophiolites in Earth History. 218. Geological Society, London, Special Publications, pp. 1–19.
- Storey, B.C., Alabaster, T., Macdonald, D.I.M., Millar, I.L., Pankhurst, R.J., Dalziel, I.W.D., 1992. Upper Proterozoic rift-related rocks in the Pensacola Mountains, Antarctica: precursors to supercontinent breakup? Tectonics 11, 1392–1405.
- Storey, B.C., Leat, P.T., Ferris, J.K., 2001. The location of mantleplume centers during the initial stages of Gondwana breakup. Mantle Plumes: Their Identification Through Time 71–80.
- Storey, B.C., Vaughan, A.P.M., Riley, T.R., 2013. The link between large igneous provinces, continental break-up and environmental change: evidence reviewed from Antarctica. Earth Environ. Sci. Trans. R. Soc. Edinburgh 104, 17–30. https://doi.org/10.1017/S175569101300011X.

- Svensen, H., Corfu, F., Polteau, S., Hammer, O., Planke, S., 2012. Rapid magma emplacement in the Karoo large igneous province. Earth Planet. Sci. Lett. 325-326, 1–9. https://doi.org/10.1016/j.epsl.2012.01.015.
- Thomson, S., Hervé, F., 2002. New time constraints for the age of metamorphism at the ancestral Pacific Gondwana margin of southern Chile. Rev. Asoc. Geol. Chile 29 (2), 255–271.
- Vaughan, A.P.M., Storey, B.C., 2000. The eastern Palmer Land shear zone: A new terrane accretion model for the Mesozoic development of the Antarctic Peninsula. Journal of the Geological Society London, 157–1256. https://doi.org/10.1144/jgs.157.6.1243.
- Vaughan, A.P.M., Leat, P.T., Dean, A.A., Millar, I.L., 2012. Crustal thickening along the West Antarctic Gondwana margin during mid-cretaceous deformation of the Triassic intraoceanic Dyer Arc. Lithos 142–143, 130–147. https://doi.org/10.1016/j. lithos.2012.03.008.
- Verard, Ch., Flores, K., Stampfli, G., 2012. Geodynamic reconstructions of the south AmericaeAntarctica plate system. J. Geodyn. 53, 43–60.
- Wever, H.E., Millar, I.L., Pankhurst, R.J., 1994. Geochronology and radiogenic isotope geology of Mesozoic rocks from eastern Palmer Land, Antarctic Peninsula: Crustal anatexis in arc-related granitoid genesis. J. S. Am. Earth Sci. 7, 69–83.
- White, R.S., McKenzie, D.P., 1989. Magmatism at rift zones: the generation of volcanic continental margins and flood basalts. J. Geophys. Res. 94, 7685–7729.
- Willner, A.P., Sepúlveda, F.A., Hervé, F., Massonne, H.J., Sudo, M., 2009. Conditions and timing of pumpellyiteactinolite-facies metamorphism in the early Mesozoic frontal accretionary prism of the Madre de Dios Archipelago (latitude 50°20'S; southern Chile). J. Petrol. 50 (11), 2127–2155. https://doi.org/10.1093/petrology/egp071.
- Zindler, A., Hart, S., 1986. Chemical geodynamics. Annu. Rev. Earth Planet. Sci. 14, 493–571